ASME
SETTING THE STANDARD

TRANSACTIONS OF THE ASME

JOURNAL OF VIBRATION AND ACOUSTICS

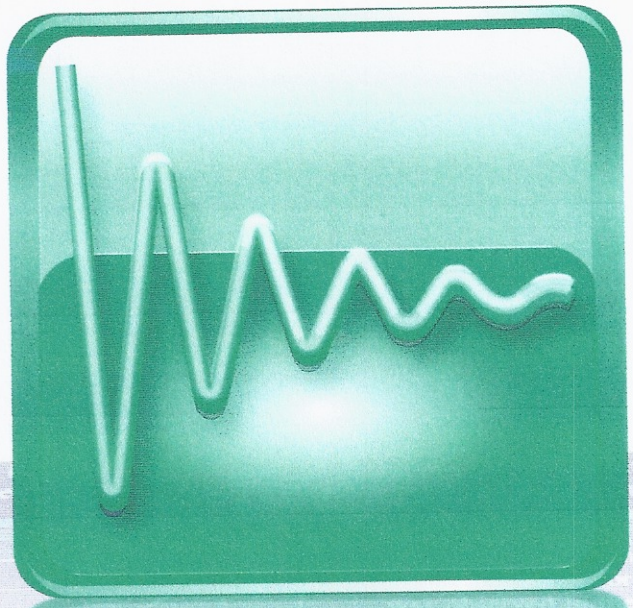

ASME JOURNALS
SETTING THE STANDARD FOR ENGINEERING KNOWLEDGE

October 2013

Load Recovery in Components Based on Dynamic Strain Measurements

Anoop K. Dhingra[1]
e-mail: dhingra@uwm.edu

Timothy G. Hunter[2]

Deepak K. Gupta

Department of Mechanical Engineering,
University of Wisconsin,
Milwaukee, WI 53201

This paper presents a modeling approach for estimating time varying loads acting on a component from experimental strain measurements. The strain response of an elastic vibrating system is written as a linear superposition of strain modes. Since the strain modes, as well as the normal displacement modes, are intrinsic dynamic characteristics of a component, the dynamic loads exciting a component are estimated by measuring induced strain fields. The accuracy of the estimated loads depends on a number of factors, such as the placement locations and orientations of the gauges on the instrumented structure, as well as the number of retained modes from strain modal analysis. A solution procedure based on the construction of D-optimal designs is implemented to determine the optimum locations and orientations of strain gauges such that the variance in load estimates is minimized. A numerical as well as an experimental validation of the proposed approach through two example problems is also presented.
[DOI: 10.1115/1.4024384]

Keywords: load recovery, force transducer, D-optimum design, gauge placement

1 Introduction

A structure responds to external loads (or moments) imposed on it with changes in quantities, such as stresses and strains, displacements, kinematic deformations, etc. This paper addresses the problem of indirect measurement of time varying loads acting on a component. In the indirect approach, instead of measuring the imposed forces directly, one measures some other quantity, such as strains, displacements, etc., that can be measured easily, and then looks for a linear relationship between the measured quantity and the applied loads. The relationship, i.e., the transfer function between the applied loads and the measured quantity, can be established numerically (e.g., using finite elements), mathematically, or experimentally.

Kinematic response measurements using displacement transducers and accelerometers are well established and well documented [1]. An alternative approach involves measurement of strains using strain gauges [2]. The need to measure strains (or stresses) to other physical quantities is apparent since these are the ultimate concern of a designer interested in ensuring structural safety. Further, since the gauges are relatively cheap, the use of strain gauges to measure dynamic forces acting on a structure has become quite popular in structural dynamics testing [2–6]. In these works, both the normal displacement modes and the strain modes are used to describe dynamic characteristics of the structure.

While the concept of modal strain was used in the mid-1980s to describe dynamic behavior of a structure, it was not until 1989 when Bernasconi and Ewins [3] presented a sound theoretical basis of modal stress/strain fields. The relationship between strain frequency response function and displacement frequency response function has also been explored by several authors [4–6]. While both the strain and displacement modes are intrinsic dynamic characteristics of a structure and correspond to each other, it has been noted in [6] that for sensitivity reasons, strain modal analysis is more useful in dynamic design of structures with features such as holes, grooves and cracks.

To illustrate the use of strain gauges for recovery of dynamic loads, many of the works mentioned above considered a simply supported cantilevered beam on which gauges were located in an ad hoc manner. While the gauge location on a straight cantilevered beam may be intuitive under certain loading conditions, the same cannot be said of a complex structure where a trial-and-error approach to gauge placement can result in poor load estimates. This is because the gauge may be placed at a location where it has a relatively low sensitivity to the load(s) to be estimated. Further, for multidegree of freedom force gauges, the cross-sensitivity [7] between the gauges may not be small. As a result, the strain data obtained from many of the gauges may be of little use, and the load estimates may not be precisely known.

For static loads, the influence of gauge locations and orientations on the quality of load estimates is discussed in [8]. However, in this work, it was noted that an analysis of all possible combinations of gauge placements would be too time-consuming for most problems. Consequently, only a few ad hoc groups of gauges were selected for analysis. If all possible gauge locations and orientations are not analyzed, the results are not guaranteed to be optimal, which in turn, may not yield the best possible load estimates.

To overcome this difficulty, Wickham et al. [9] cast the gauge location problem as an optimization problem wherein the determination of optimum values for gauge locations and orientations was done for a C-spring. However, the proposed technique was demonstrated for recovery of static and quasi-static loads, and needs to be generalized to handle complex 3-D structures, which have vibration inducing loads imposed on them. Recently, a genetic algorithm based approach for mounting strain gauges on turbine blades to capture vibration modes has also been presented [10,11]. However, this approach is limited to the recovery of mode shapes, and not the loads acting on a component.

To overcome the shortcomings mentioned above, this paper outlines an approach for formulating and solving the gauge placement problem when the imposed loads being estimated induce vibrations in the structure, resulting in time varying dynamic strains. The accuracy of load estimates is dependent on the placement (location and orientation) of the strain gauges, and the number of strain modes retained in the analysis. A sequential

[1]Corresponding author.
[2]Currently President, Wolf Star Technologies, 3321 N. Newhall St., Milwaukee, WI 53211, e-mail: tim.hunter@wolfstartech.com.
Contributed by the Design Engineering Division of ASME for publication in the JOURNAL OF VIBRATION AND ACOUSTICS. Manuscript received March 5, 2012; final manuscript received April 26, 2013; published online June 18, 2013. Assoc. Editor: Jean Zu.

exchange algorithm based approach [12,13] is used to select the optimum locations, and angular orientations of the strain gauges. Two examples, one dealing with an experimental validation of proposed procedures and the other dealing with a numerical validation of the proposed approach, are presented.

2 Mathematical Foundations

Consider first the problem of estimating k quasi-static loads acting on a component by using m ($m \geq k$) strain gauges mounted on the component surface. If the deformations are small enough so that the superposition principle holds, then the strain at any location on the component is written as

$$\varepsilon = AF \tag{1}$$

Here ε is an $m \times 1$ vector of strains, A is an $m \times k$ matrix of sensitivity coefficients, and F is a $k \times 1$ vector of loads. Assuming that the sensitivity matrix A is known and the strain values ε are measured, the unknown load vector (F) can then be estimated as [8]

$$\hat{F} = \left(A^T A\right)^{-1} A^T \varepsilon \tag{2}$$

Here $\hat{F}$ denotes a least-squares estimate of unknown load F. If the errors in strain measurements are statistically independent and the standard deviation of each one is σ, then the covariance matrix for load estimates is [8]

$$\text{var}\,\hat{F} = \sigma^2 (A^T A)^{-1} \tag{3}$$

The smaller the variance of the load estimates, the better the precision with which the loads are estimated. Therefore, the uncertainty in load estimates can be minimized by ensuring that the matrix $(A^T A)^{-1}$ is well behaved. It is well known that maximizing the determinant of $A^T A$ yields the best possible estimates for the load vector (F) [12–14]. Such designs are called D-optimal.

Considered next is the problem when the imposed load $F(t)$ is time varying and induce vibrations in the component. The equations of motion (EOM) for an n-DOF vibrating system are given as

$$[M]\{\ddot{x}\} + [K]\{x\} = \{F(t)\} \tag{4}$$

where $x(t)$ is a $n \times 1$ vector. The free vibration response of this system can be written as a linear combination of the normal modes as follows:

$$\{x(t)\} = \sum_{i=1}^{n} q_i(t)\phi_i = [\Phi]\{q(t)\} \tag{5}$$

Here $q_i(t)$ is the mode participation factor (MPF) for mode ϕ_i Defining the $n \times n$ modal matrix for free vibrations as $[\Phi] = [\phi_1, ..., \phi_n]$, the decoupled EOM for the ith MPF can be written as

$$\ddot{q}_i + \omega_i^2 q_i = (\Phi^T F)_i \tag{6}$$

Likewise, for a damped system with input force $F(t)$, the EOM are

$$[M]\{\ddot{x}\} + [C]\{\dot{x}\} + [K]\{x\} = \{F(t)\} = \{Fe^{i\bar{\omega}t}\} \tag{7}$$

For a harmonic response, $x(t) = Xe^{i\bar{\omega}t}$, one gets

$$\begin{aligned}[X] &= \left[K - M\bar{\omega}^2 + iC\bar{\omega}\right]^{-1}[F] \\ &= [\alpha(\bar{\omega})][F]\end{aligned} \tag{8}$$

It may be noted that $\alpha(\bar{\omega})$ as defined in Eq. (8) is called the displacement frequency response function (DFRF) or the receptance matrix. In terms of modal coordinates, the EOM are given as

$$[M][\Phi][\ddot{q}(t)] + [C][\Phi][\dot{q}(t)] + [K][\Phi][q(t)] = F(t) \tag{9}$$

For a structural continuum, the strains and displacements $\{x(t)\}$ at any point in a structure are related as

$$\{\varepsilon\} = D\{x\} \tag{10}$$

where D is a differential operator. Application of the differential operator to the physical response $\{x(t)\}$ expressed as a linear superposition of the modes (Eq. (5)) at a particular instant of time gives

$$D(\{x(t)\}) = D([\Phi])\{q(t)\} \tag{11}$$

which leads to

$$\{\varepsilon(t)\} = [\Psi^{\varepsilon}]\{q(t)\} \tag{12}$$

Here $[\Psi^{\varepsilon}]$ is called the modal strain matrix and contains the strain modes of the structure. Equation (12) states that for a particular time, the strain response can be expressed as a linear combination of the modal strains. The modal strains are an intrinsic property of structure's dynamic behavior, as are the displacement mode shapes.

Assuming that $[\Psi^{\varepsilon}]$ is known and $\{\varepsilon(t)\}$ is measured, the least squares estimate of the MPF $\{q(t)\}$ is given as

$$\{q(t)\} = \left([\Psi^{\varepsilon}]^T [\Psi^{\varepsilon}]\right)^{-1} [\Psi^{\varepsilon}]^T \{\varepsilon(t)\} \tag{13}$$

Once the MPF $\{q(t)\}$ are calculated using Eq. (13), the response $\{x(t)\}$ is known (Eq. (5)) and the imposed forces can be estimated using Eqs. (4) or (7).

Presented next is an outline of the solution approach that will allow for the estimation of time varying loads $\{F(t)\}$ acting on the component by measuring strains at a finite number of locations. The gauge orientations and locations will be optimized such that the loads estimates are as precise as possible. These locations and orientations are determined using a sequential exchange algorithm [13] first proposed in the context of optimal design of experiments.

3 Gauge Placement Problem

In the context of gauge placement, to achieve the best estimates for the loads $F(t)$, D-optimal designs help determine (i) where on the surface of the structure should gauges be mounted, (ii) at what angle should these gauges be mounted, and finally (iii) how many gauges should be used. To determine D-optimal designs from a set of candidate gauge locations and orientations, it is essential that the sensitivity matrix A (see Eq. (1)) be established first.

The steps involved in generating the sensitivity matrix A are as follows. First, a finite element (FE) model of the component to be instrumented is created. Since the strain gauges will be mounted on the component's surface, the elements used for FE modeling should allow for availability of surface strain information at locations where gauges could be mounted. From a practical standpoint and to avoid errors due to strain approximations, the FE meshing should be done such that the element size is compatible with the physical dimensions of the strain gauge that will be located on the surface.

Next, a unit load is applied to the component corresponding to each load to be estimated. The resulting strain field from each of the load conditions is computed, in local (element frame of reference) and global coordinate systems at all candidate locations. The finite element analysis results are used, along with strain transformation relations, to generate the strain response at each element, for each possible of strain gauge angular orientation $\theta, 0 \leq \theta \leq 180$.

Since the gauge sensitivity varies as the gauge orientation changes, the strain tensor is transformed to determine strain values for different gauge orientations as follows [15]:

$$[\varepsilon]_{x'y'z'} = [T][\varepsilon]_{xyz}[T]^T \tag{14}$$

Here T denotes the transformation matrix and contains the direction cosines for the $x'y'z'$ system relative to the xyz coordinate system. For the shell elements used herein to prepare the FE model, the element z-axis is always normal to the element. Therefore, the strain transformations involve rotation about the z-axis with the transformation matrix T given as

$$[T] = \begin{bmatrix} \cos\theta & \sin\theta & 0 \\ -\sin\theta & \cos\theta & 0 \\ 0 & 0 & 1 \end{bmatrix} \tag{15}$$

By varying θ, the strain tensor at intermediate gauge orientations can be obtained.

Each combination of strain gauge location and angular orientation is a candidate point for inclusion in the A matrix. The terms in each row of the A matrix represent the response of a strain gauge, at a particular location and angular orientation, to each individual load. From this set of candidate gauge locations and orientations, a subset of m gauges is selected randomly. Given this m-gauge design, each candidate gauge location (y) currently not selected is adjoined to the A matrix. The determinant of the adjoined matrix (M^+) with $m+1$ gauges is given as [12]

$$\det M^+ = \det M * (1 \pm y^T M^{-1} y) \tag{16}$$

The row leading to largest increase in det M^+ is retained and the inverse of M^+ is updated as [12]

$$(M^+)^{-1} = M^{-1} \mp (M^{-1}y)(M^{-1}y)^T/(1 \pm y^T M^{-1} y) \tag{17}$$

In Eq. (16), $\pm$ should be replaced by plus when a gauge is being added, and by minus when a gauge is being deleted. A similar argument applies to the $\mp$ term in Eq. (17). From the $m+1$ gauge design, a gauge is deleted which results in the smallest reduction in det M^+ This process of adding and removing most and least sensitive gauges continues until det M cannot be improved further. In this work, the sequential exchange procedure [13] outlined above along with computational improvements proposed by Galil and Keifer [12] are implemented. A computer implementation of these algorithms was done in a MATLAB® programming environment.

Once the gauge locations and orientations are determined on the surface of the component, the next step involves transforming the gauge-orientation information from the local space (element coordinate system) to the global x-y-z space. The global gauge orientation is needed in order to physically lay the gauge on the actual component. In order to accomplish this objective, the invariance of local and global principal strains is utilized. Since principal strains at any point on the component are invariant with respect to coordinate transformations, an eigenvalue problem is solved to determine the relationship between local and global gauge orientation direction cosine vectors. This, in turn, will yield the global direction cosine vector for the gauge orientation.

Let ε_L and ε_G, respectively, denote the local and global strain tensors at an element. The principal strains (for strain tensor H) are obtained by solving the eigenvalue problem,

$$\begin{aligned} Hx &= \lambda x \\ x^T H x &= \lambda x^T x \end{aligned} \tag{18}$$

Here λ denotes the eigenvalues or principal strains and x denotes the eigenvectors or the principal directions. If the eigenvectors are normalized such that $x^T x = 1$, then writing the above eigenvalue problem for local and global strain tensors yields

$$\begin{aligned} V_L^T \varepsilon_L V_L &= \lambda_L \\ V_G^T \varepsilon_G V_G &= \lambda_G \end{aligned} \tag{19}$$

Due to invariance of the principal strains, $\lambda_L = \lambda_G$, giving

$$V_L^T \varepsilon_L V_L = V_G^T \varepsilon_G V_G \tag{20}$$

Premultiplying the above equation by V_G and postmultiplying by V_G^T yields

$$V_G V_L^T \varepsilon_L V_L V_G^T = \varepsilon_G \tag{21}$$

Letting $T_m = V_G V_L^T$ results in

$$\varepsilon_G = T_m \varepsilon_L T_m^T \tag{22}$$

Thus the transformation matrix T_m can be used to transform tensors as well as vectors between the local and the global coordinate systems.

If the optimum gauge orientation in the element space corresponds to a gauge orientation angle θ with respect to the element's local x-axis, then a unit vector corresponding to gauge orientation is given as $X_L = [\cos(\theta), \sin(\theta), 0]^T$. The global direction cosine vector, for the gauge orientation, can now be calculated as

$$X_G = T_m X_L \tag{23}$$

This global direction cosine vector information can be imported back in the FE software so that the gauge locations can be superimposed on the FE mesh for ease of visualization (see Fig. 3 below).

Lastly, the issue pertaining to the number of required strain gauges is addressed. It may be noted that when attempting to estimate k loads (or MPF), the number of gauges (m) used must satisfy the relation $m \geq k$.

If ε_{ei} denotes the strain reading from gauge i (experimentally measured value) and ε_{pi} denotes the predicted strain for gauge i with $\{\varepsilon_p\} = [A]\{f\}$, then the estimation error for gauge i is given as $e_i = \varepsilon_{ei} - \varepsilon_{pi}$ and for an overconstrained system of linear equations with $n-m$ degrees of freedom, the variance of strain measurement errors is given as [16]

$$\sigma^2 = \frac{\sum_{i=1}^{m} e_i^2}{m-k} \tag{24}$$

4 Solution Procedure

Summarized next are the steps involved in the recovery of dynamic loads acting on a component which has a finite number of strain gauges located on the component to measure time varying strains.

i. Construct a finite element model of the component and perform its modal analysis to determine component's natural frequencies and mode shapes.
ii. Next, decide how many normal modes will be retained to approximate the structural response. Let r denote the number of kept modes. The fraction of modal mass captured by r kept modes can be used to adjust r so that structural response is reasonably approximated using r modes.
iii. Determine the strain field corresponding to each retained normal mode of the component. These yield the strain modes $[\Psi^e]$ of the structure.
iv. Use the strain field information from step (iii) to determine optimum gauge locations and orientations. The number of gauges employed (m) should be greater than or equal to r.
v. Next, given the experimental strain field from a component on which the gauges are mounted as outlined in step (iv), the load recovery step (Eq. (13)) yields the participation factor of each strain mode in the overall strain response.
vi. With the MPF known, the displacement $\{x(t)\}$ is approximated using Eq. (5) and eventually the imposed force $F(t)$

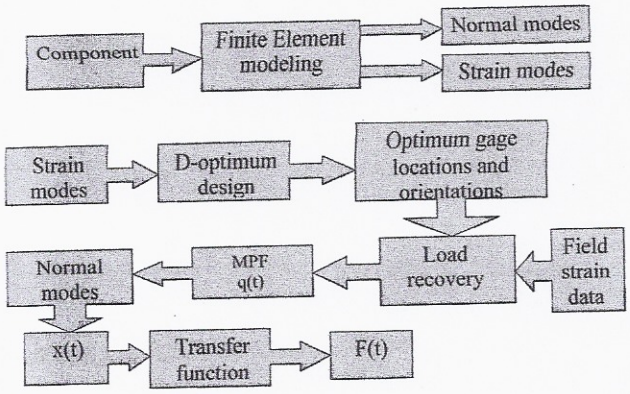

Fig. 1 Flow chart of the overall solution process

can be recovered using the DFRF. Alternately, the displacement $\{x(t)\}$ can be used in conjunction with Eq. (7) to recover $F(t)$.

A complete flow chart of the solution approach is given in Fig. 1.

5 Examples

Presented next are two examples, one numerical and one experimental, which illustrate the applicability of the proposed procedure for load recovery in cantilevered beams. The first example

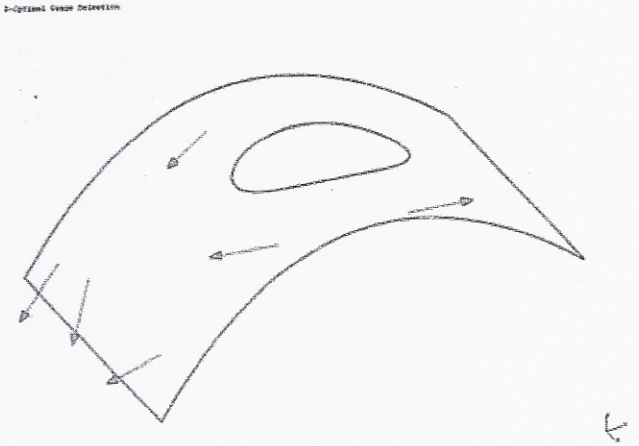

Fig. 3 Optimum gauge locations and orientations

deals with the recovery of three arbitrary loads acting on a bent cantilevered beam. The second example deals with experimental validation of proposed procedures on a cantilevered beam subject to a base excitation.

5.1 Example 1. Consider the bent cantilevered beam shown in Fig. 2 with an elliptical hole in the center. This beam was modeled in I-DEAS® software and the first four natural frequencies and mode shapes were computed. The mode shapes are

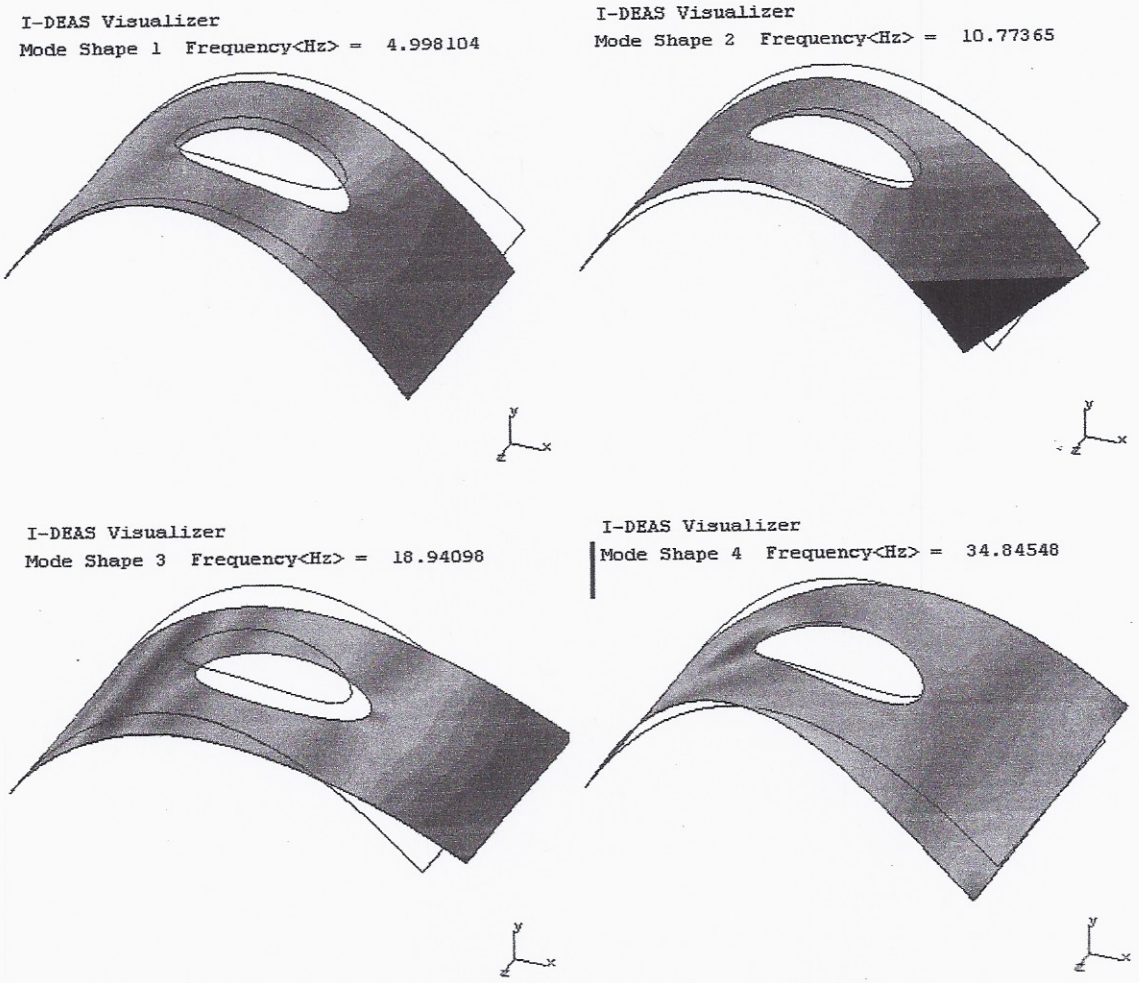

Fig. 2 Bent beam with its four modes

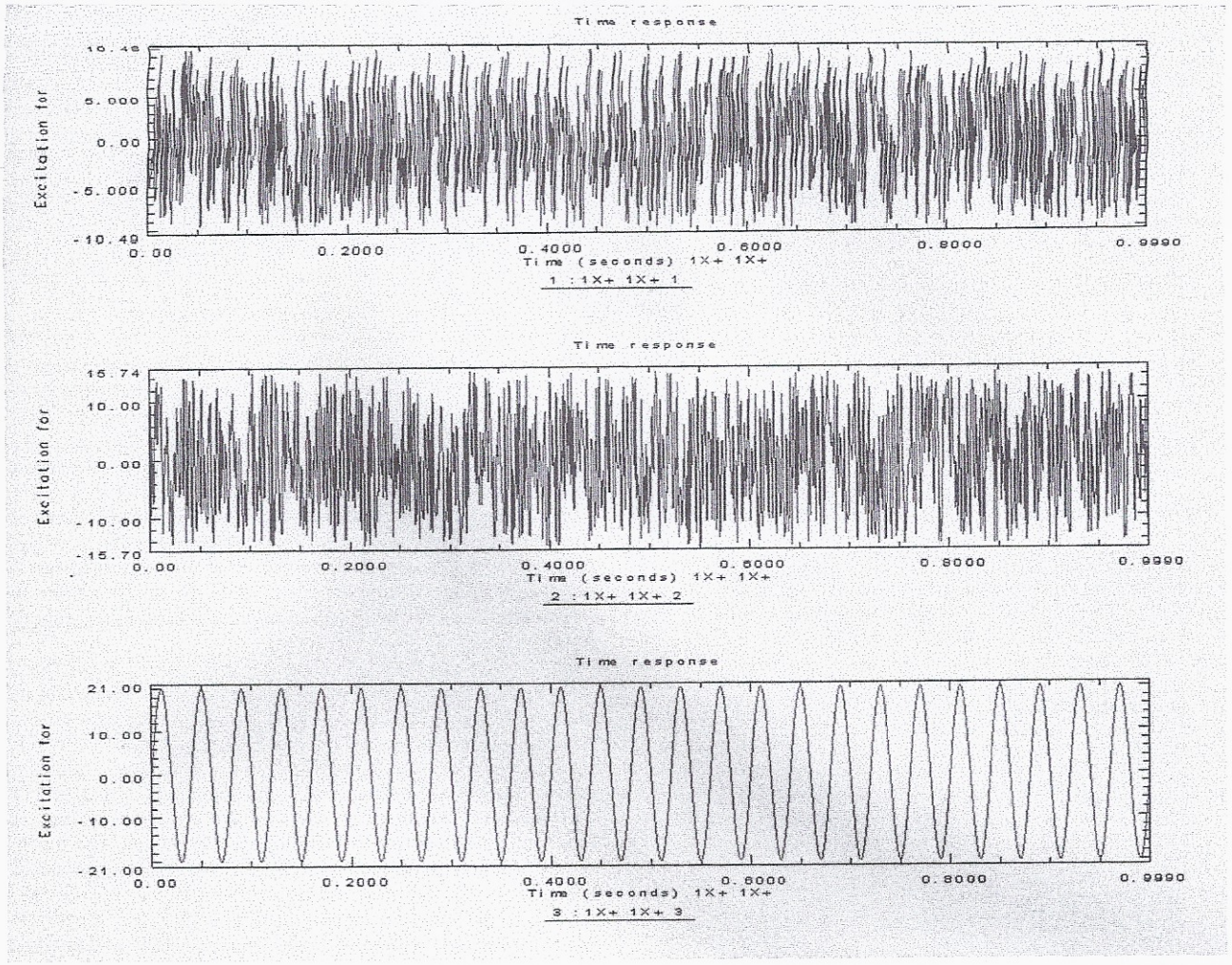

Fig. 4 Load-time history applied at the tip of the beam

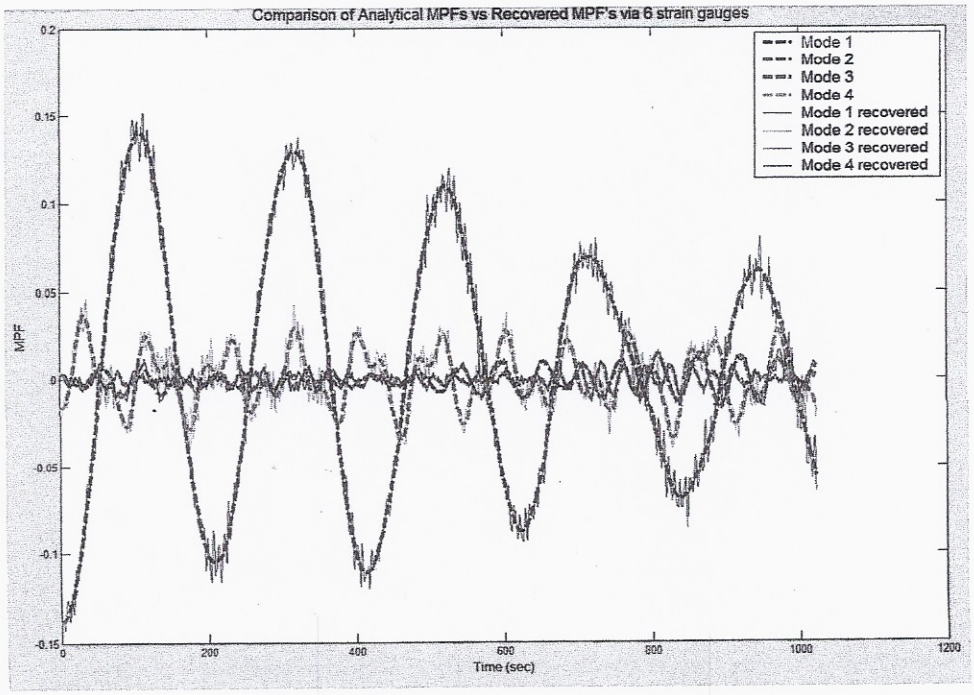

Fig. 5 Recovered mode participation factors

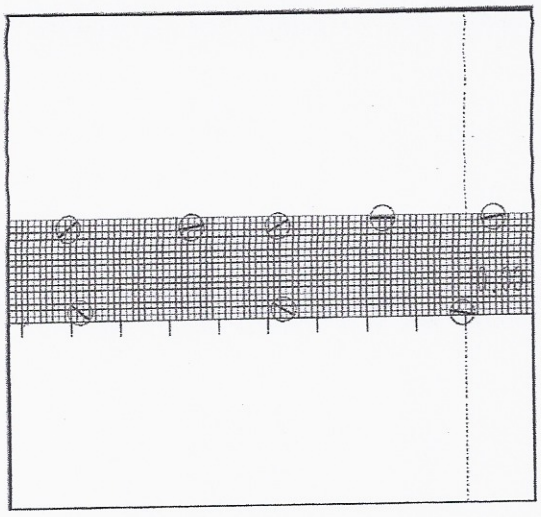

Fig. 6 Cantilevered beam with optimum gauge placement

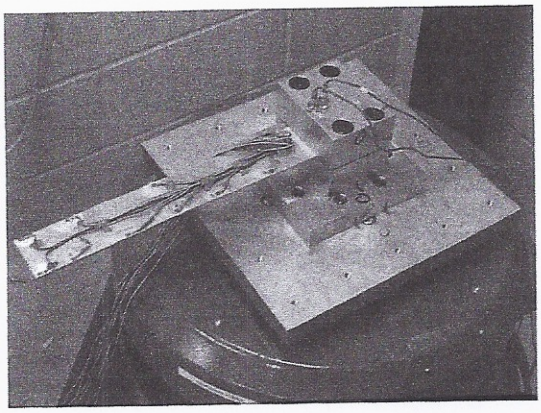

Fig. 7 Clamped cantilevered beam mounted on the shaker

Table 1 Beam with a 28 Hz base excitation

28 Hz dwell	Experimental MPF		Theoretical MPF	
Mode	MPF	Particip. %	MPF	Particip. %
1	1.87×10^{-2}	94.9	1.16×10^{-1}	99.98
2	-5.63×10^{-4}	2.8	1.62×10^{-5}	0.01
3	-3.28×10^{-4}	1.7	-2.42×10^{-14}	0.00
4	4.77×10^{-6}	0.0	-5.00×10^{-19}	0.00
5	9.78×10^{-5}	0.5	1.14×10^{-6}	0.00

normalized to yield a unit-mass matrix. The four mode shapes are shown in Fig. 2. It was seen that four modes are sufficient to capture the overall response of this continuous system. For this example with four retained normal modes, at least four gauges are needed to recover the external loads acting on the beam. Since the required number of gauges is greater than the numbers of retained modes, a total of six gauges (number selected arbitrarily) are used. The optimum gauge locations and orientations for a 6-gauge design chosen here are given in Fig. 3. It may be noted that the local to global transformation of optimum gauge orientations was done using Eq. (23) before the gauge orientations are superimposed on Fig. 3.

Next, three time varying loads (see Fig. 4) are applied to the upper right-hand corner of the cantilevered beam. The strain field resulting from the loading in Fig. 4 is input to the load recovery module and the MPF for all four modes are computed. A time history of these MPF is given in Fig. 5. A modal analysis of the content of the three superimposed input signals is also performed using I-DEAS® to determine the MPF for the input loading. The recovered and the imposed MPF for all four modes, as a function of time, are also shown in Fig. 5. Based on the results obtained, it can be seen that the proposed approach helps recover the modal content of the imposed loading such that the main contributing mode is recovered within 5% error. Once the MPF are known, the response $x(t)$ was reconstructed using Eq. (5), $\dot{x}(t)$ and $\ddot{x}(t)$ were

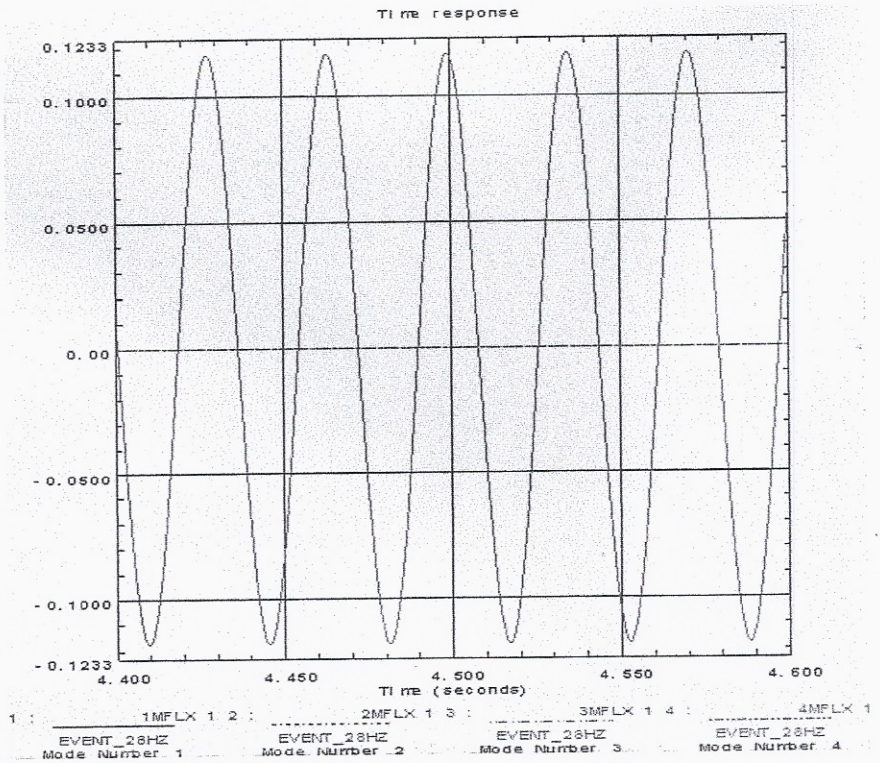

Fig. 8 MPF for a 28 Hz base excitation

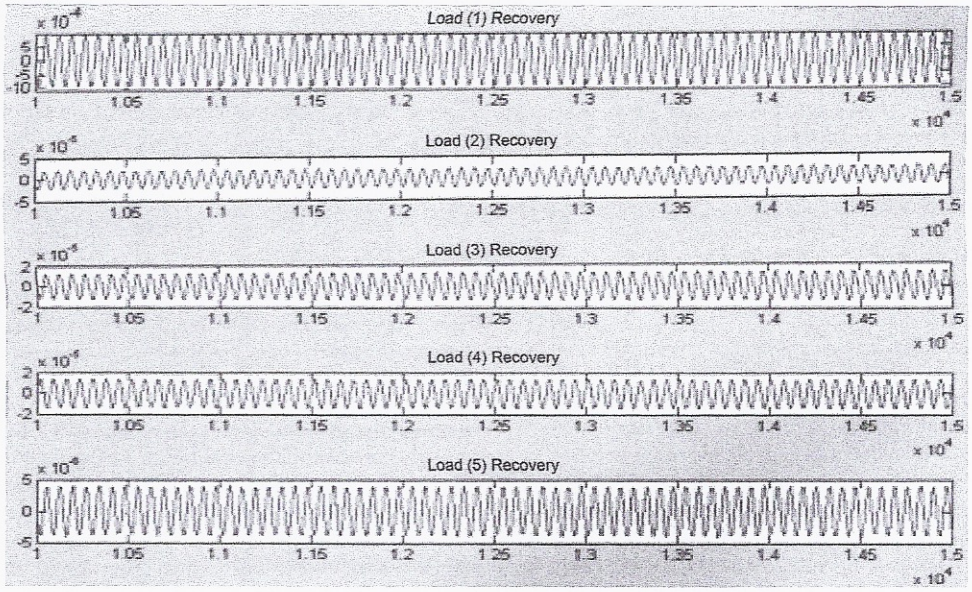

Fig. 9 Recovered MPF for a 28 Hz input

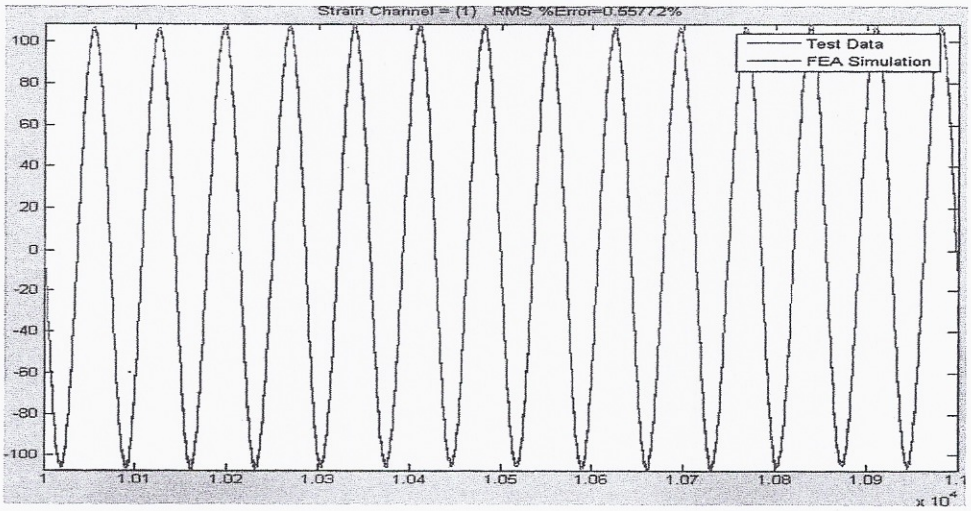

Fig. 10 Actual and reconstructed strains in gauge 1

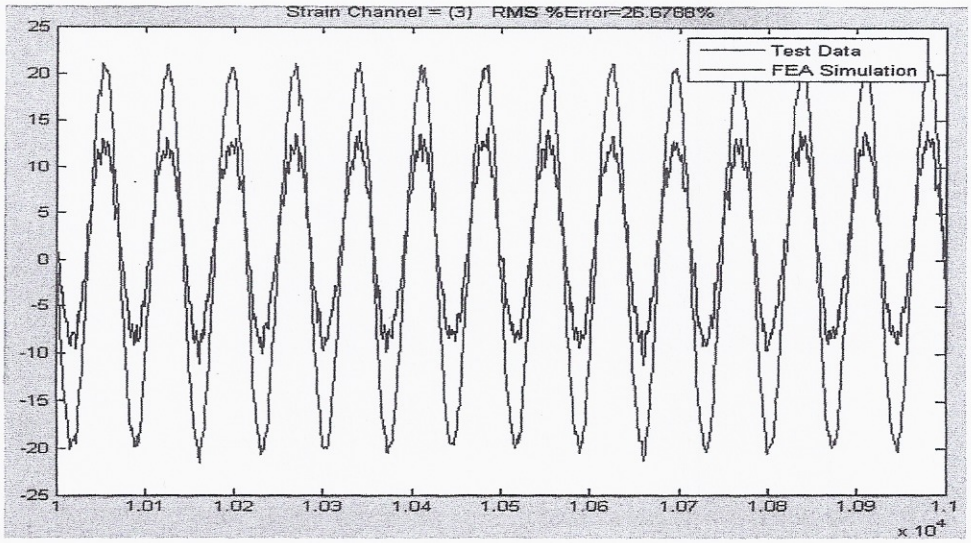

Fig. 11 Actual and reconstructed strains in gauge 3

Table 2 Beam with a 171 Hz base excitation

171 Hz dwell	Experimental MPF		Theoretical MPF	
Mode	MPF	Particip. %	MPF	Particip. %
1	-6.50×10^{-4}	6.4	-5.60×10^{-3}	11.03
2	-8.80×10^{-3}	87.0	4.49×10^{-2}	88.40
3	3.06×10^{-4}	3.0	-6.50×10^{-12}	0.00
4	-2.12×10^{-5}	0.2	-1.14×10^{-16}	0.00
5	3.25×10^{-4}	3.0	2.51×10^{-4}	0.49

computed by differentiating Eq. (5) with respect to time, and $F(t)$ was computed by using Eq. (7).

5.2 Example 2. A 12 in. long, 2 in. wide, and 1/8 in. thick cantilevered aluminum beam was modeled in I-DEAS® and the first five normal modes were retained for analysis. Of these five modes, the third mode is a twist mode, whereas the other four modes induce lateral vibrations in the beam. A total of eight gauges (arbitrarily selected number >4) were mounted on the beam and the optimum gauge locations and orientations are shown in Fig. 6. The beam was clamped at the base and attached to a shaker head (see Fig. 7).

Two input base excitations, namely a 28 Hz sine dwell and a 171 Hz sine dwell were input into the shaker head and the fixture to excite the structure. The strains at each drive input were measured and analyzed to arrive at the mode participation factors. Since the 28 Hz excitation is very close to the fundamental frequency of the beam (28.178 Hz), mode 1 dominates the overall response and overshadows all other modes by close to two orders of magnitude. This is borne out by the results given in Fig. 8 and Table 1. Figure 8 gives the MPF for the input 28 Hz loading for all normal modes, whereas Fig. 9 illustrates the recovered participation factors for all modes. The scale of the MPF for mode 1 in Fig. 9 is one order of magnitude higher than those for modes 2–5. The numerical values in Table 1 are taken at an instant of time, and give a snapshot of various MPF at the chosen time. It can be seen from the results in Table 1 that mode 1 dominates all other modes, and its participation percentage is recovered within 5% of the theoretical value. It may be noted that since mode shapes are known up to a constant, the MPF from FEA and from proposed load recovery procedure cannot be compared directly on a one-to-one basis. To resolve this ambiguity regarding the mode shapes and MPF, the participation percentages are compared. It is seen from Table 1 that the participation percentages of all modes are in good agreement with the theoretical values.

An additional check on the recovery procedure as outlined herein includes correlating the measured and predicted strains in various gauges mounted on the beam. Figure 10 shows that the strain in gauge 1 is reproduced within 0.56% error, whereas for gauge 3, the strain error is of the order of 5-10 microstrains (Fig. 11). The error for gauge 3 was within the experiment's measurement limit of about 10 microstrains.

Next the beam is excited by a 171 Hz sine dwell which is not too far from the second frequency of 176.34 Hz. For this case, mode 2 dominates the overall response because the 171 Hz excitation is closer to the second frequency of the beam of 176.35 Hz. The mode participation factors for all modes were computed and numerical values at a particular instant in time are given in Table 2. It was seen that MPF are recovered reasonably accurately. With the MPF known, the response $x(t)$ was reconstructed using Eq. (5), $\dot{x}(t)$ and $\ddot{x}(t)$ were computed by differentiating Eq. (5), and $F(t)$ was computed by using Eq. (7).

6 Conclusions

A computational methodology is presented that allows for indirect measurement of dynamic loads imposed on a component. This is done by placing strain gauges on the structure such that best possible load estimates are obtained from the measured strain information. To improve the precision of load estimates, optimum design of experiment techniques in conjunction with finite element analysis is used to determine values for gauge locations and orientations. Numerical results on two examples illustrate the effectiveness of the proposed approach in recovering time varying loads which induce significant levels of vibrations in the component. The examples show that the participation percentage of the dominant mode is recovered within 5% of the theoretical value. The MPFs of the first few retained modes were successfully reconstructed from the system response. The reconstructed strain in dominant gauge (gauge 1) is with 0.56% of the actual strain. It was also noted that the strain error in less dominant gauges was of the order of 5–10 microstrains which was within the experiment's measurement limit.

In more complex and real world problems, only a few modes are available most of the time. This may lead to errors due to mode truncation. Recovery of large number of MPFs would require more strain gauges to be used, which may not always be feasible. Future research will focus on these areas so as to obtain the highest accuracy with fewer available modes.

Acknowledgment

The work was supported in part through funds provided by Harley-Davidson Motor Company, UW Applied Research Grant program, and a UWM RGI award. This support is gratefully acknowledged.

References

[1] Ewins, D. J., 2000, *Modal Testing: Theory, Practice, and Applications*, Research Studies Press Ltd., Baldock, UK.
[2] Hillary, B., and Ewins, D. J., 1984, "The Use of Strain Gages in Force Determination and Frequency Response Function," Proceedings of the 2nd International Modal Analysis Conference (IMAC), Orlando, FL, February 6–9, pp. 627–634.
[3] Bernasconi, O., and Ewins, D. J., 1989, "Modal Strain/Stress Fields," J. Modal Anal., 4(2), pp. 68–76.
[4] Li, D. B., Zhuge, H., and Wang, B., 1989, "The Principles and Techniques of Experimental Strain Modal Analysis," Proceedings of the 7th International Modal Analysis Conference (IMAC), Las Vegas, NV, January 30-February 2, pp. 1285–1289.
[5] Tsang, W. F., 1990, "Use of Dynamic Strain Measurements for the Modeling of Structures," Proceedings of the 8th International Modal Analysis Conference (IMAC), Kissimmee, FL, January 29-February 1, pp. 1246–1251.
[6] Yam, L. H., Leung, T. P., Li, D. B., and Xue, K. Z., 1996, "Theoretical and Experimental Study of Modal Strain Analysis," J. Sound Vib., **191**(2), pp. 251–260.
[7] Sommerfeld, J. L., and Meyer, R. A., 1999, "Correlation and Accuracy of a Wheel Force Transducer as Developed and Tested on a Flat-Trac® Tire Test System," SAE Paper No. 1999-01-0938.
[8] Masroor, S. A., and Zachary, L. W., 1990, "Designing an All-Purpose Force Transducer," Exp. Mech., **31**(1), pp. 33–35.
[9] Wickham, M. J., Riley, D. R., and Nachtsheim, C. J., 1995, "Integrating Optimal Experimental Design Into the Design of a Multi-Axis Load Transducer," ASME J. Eng. Ind., **117**(3), pp. 400–405.
[10] Szwedowicz, J., Senn, S. M., and Abhari, R. S., 2002, "Optimum Strain Gage Application to Bladed Assemblies," ASME J. Turbomach., **124**(4), pp. 606–613.
[11] Mignolet, M. P., and Choi, B. K., 2003, "Robust Optimal Positioning of Strain Gages on Blades," ASME J. Turbomach., **125**(1), pp. 155–164.
[12] Galil, Z., and Kiefer, J., 1980, "Time- and Space-Saving Computer Methods, Related to Mitchell's DETMAX, for Finding D-Optimum Designs," Technometrics, **22**(3), pp. 301–313.
[13] Mitchell, T. J., 1974, "An Algorithm for the Construction of D-Optimal Experimental Designs," Technometrics, **16**(2), pp. 203–210.
[14] Atkinson, A. C., and Donev, A. N., 1992, *Optimum Experimental Designs*, Oxford University Press, New York.
[15] Budynas, R. G., 1999, *Advanced Strength and Applied Stress Analysis*, 2nd ed., McGraw-Hill, New York.
[16] Chatterjee, S., and Hadi, A. S., 1988, *Sensitivity Analysis in Linear Regression*, John Wiley, New York.